Fractal Analysis of Morphology of PE/PA Blends: Composition

Xu-Huang Chen,[1,2] Wen-Xiong Shi,[1] Shi-Hai Yang,[1] Yun-Yan Li,[1] Gui-Qiu Ma,[1] Jing Sheng[1]

[1]*School of Material Science and Engineering, Tianjin University, Tianjin 300072, China*
[2]*School of Chemical and Environmental Engineering, Hubei University of Technology, Wuhan 430068, China*

Received 19 June 2007; accepted 10 November 2007
DOI 10.1002/app.27833
Published online 9 May 2008 in Wiley InterScience (www.interscience.wiley.com).

ABSTRACT: Composition effect on the phase morphology in polyethylene (PE) with polyamide (PA) blends was investigated by pattern analysis of scanning electron micrographs. The average diameter denoted as d_g is defined to discuss the morphology of the blends and further, different fractal dimensions, D_M and D_N, were introduced to characterize the phase morphology. Scale function $S_N(r)$ and $S_M(r)$ are defined to study the selfsimilarity of the phase morphology. The plots of $S_N(r)/S_N(r)m$ (the maximum of $S_N(r)$) versus r/rm (the maximum of r) and $S_M(r)/S_M(r)m$ (the maximum of $S_M(r)$) versus r/rm showed the selfsimilar formation of the phase pattern. Furthermore, we calculated the fractal dimension D of different PE/PA blends. The results showed that the fractal dimension was an effective parameter to describe the spacial distribution of dispersed particles. © 2008 Wiley Periodicals, Inc. J Appl Polym Sci 109: 2496–2502, 2008

Key words: polymer blends; polyethylene; polyamide; fractal character of polymer blends

INTRODUCTION

Since the morphology of the polymer blends has a significant influence on its mechanical properties, the mechanism of morphology has attracted more interests from both academic and commercial institutes. During the past few decades, many research groups carried out corresponding studies to gain a better understanding of morphology and good results were found.[1–6] It is well known that when two immiscible/imcompatible polymers are blended, one phase will mechanically disperse into the other and form the dispersed phase, while the other becomes the continuous phase. In general, the particle size of the minor phase depends greatly on the composition, the viscoelasticity of the constituent components, the shear stress/rate and the interfacial tension between phases. Therefore, the phase morphology can be controlled by adjusting processing conditions (such as the mixing temperature, the rotor speed, and so on).

To get materials with preeminent performance, the phase morphology during melting and mixing has been researched by many people. Sailer and Handge[7] studied the morphology of PA6/SAN with rheological behavior. Using a mixer, Sheng and coworkers[8–11] investigated the phase morphology in the initial stage of the blending process and found SALS was an effective method to blend. Plivelic et al.[12] investigated the morphology of PCL/PECL by DSC, simultaneous SAXS/WAXD, and elemental mapping by ESI-TEM. However, there are few reports of study on the phase morphology based on the fractal theory.

Blends of polyethylene (PE) with polyamide (PA) may lead to polymers possessing a synergic combination of the typical properties of PE, namely, low cost, processability, resilience, and moisture insensitivity, with those of PA, i.e., rigidity, thermal stability, and barrier properties to oxygen and solvents[13–17]. In this article, the composition effect on the phase morphology in PE/PA incompatible blends was investigated by analyzing the scanning electron micrographs (SEM) based on the fractal theory, which will accelerate the industrialization of PE/PA blend.

THEORY

Figure-estimation theory of logarithm-normal distribution

In the present work, the figure-estimation theory[18] is introduced to judge whether the distribution of a variable is the logarithm-normal distribution. If the logarithm in the log normal distribution is a common logarithm, the distribution function can be defined as

Correspondence to: G.-Q. Ma (magq@tju.edu.cn) or J. Sheng (ghxu@tju.edu.cn).

Contract grant sponsor: National Natural Science Foundation; contract grant number: 50390090 and the Science Technology Committee of Tiangin, China; grant number: 05YFJMJCOG100.

© 2008 Wiley Periodicals, Inc.

$$F(t)=\frac{\lg e}{\sqrt{2\pi}\sigma t}\int_{-\infty}^{t}\exp\left[-\frac{1}{2}\left(\frac{\lg t-\mu}{\sigma}\right)^2\right]dt \quad \text{for } t\in[0,+\infty] \tag{1}$$

Here σ and μ are the standard deviation and number average of the distribution in ln(t), respectively. A large σ often corresponds to a wide distribution. The distribution function is a monotonic ascending curve in the t∼F(t) coordinate system. It can be transformed into the expression of the standard normal distribution as follow:

$$F(t)=\int_{-\infty}^{\frac{\lg t-\mu}{\sigma}}\frac{1}{\sqrt{2\pi}}e^{-\frac{x^2}{2}}dx=\Phi\left(\frac{\lg t-\mu}{\sigma}\right) \quad \text{for } t\in[0,+\infty] \tag{2}$$

Because the standard normal distribution function, $\Phi(X)$, is strictly monotonic ascending, its inverse function exists. The inverse function can be defined as:

$$\Phi^{-1}[F(t)]=\frac{\lg t-\mu}{\sigma} \tag{3}$$

If let $Y = \Phi^{-1}[F(t)]$ and $X = \ln t$, the inverse function turns to be

$$Y=\frac{1}{\sigma}X-\frac{\mu}{\sigma} \tag{4}$$

This is a linear equation in the *X*–*Y* coordinate system. Its slope, which is positive, is $1/\sigma$. Its interception is μ/σ. Thus, a log-normal distribution curve corresponds to an ascending line in the *X*–*Y* coordinate system. Correspondingly, an ascending line in the *X*–*Y* coordinate system will indicate a log-normal distribution function. It is clear that a one by one relation between the ascending line in the *X*–*Y* coordinate system and the log-normal distribution function can be established.

Fractal theory by fractal measure relations

For a set of points distributed in space, the fractal dimension can be defined in the following manner.[19,20] Thinking of a sphere of radius, *r*, we can denote the number of points which are included in the sphere by $M(r)$. If the points fall on a straight line and are distributed uniformly, $M(r)$ will be proportional to *r*, $M(r) \propto r$. If the distribution of points is plane-like, then $M(r) \propto r^2$, for points distributed uniformly over three-dimensional space, $M(r)$ will be proportional to r^3, by generalizing these relations we may say the fractal dimension of the points' distribution is *D* and that

$$M(r)\propto r^D \tag{5}$$

is satisfied. Formula (5) can be changed to

$$D=\frac{\log M(r)}{\log r} \tag{6}$$

So the fractal dimension can be obtained by plotting $\log M(r)$ against $\log r$.

To distinguish the two different phases on SEM micrographs, the SEM micrographs of samples for different compositions were binarized. The particles of the dispersed phase can be regarded as a set of points distributed on a plane according to this theory, we can draw a square, noting the length of the square's border, *r*, and the number of the dispersed particles included in the square $M(r)$. For a certain *r*, changing the position of the square on the SEM micrograph, we can get a set of number of the dispersed particles: $M(r)_1$, $M(r)_2$, $M(r)_3$,...$M(r)_n$. To obtain better statistical sense, we define the number of the dispersed particles included in the square of a certain border length $M(r)$ by Formula (7):

$$M(r)=\sqrt[n]{M(r)_1M(r)_{21}M(r)_3\cdots M(r)_n} \tag{7}$$

By changing the length of the square's border, we may obtain a set of different $M(r_i)$, and the fractal dimension, *D*, can be obtained by plotting $\log M(r)$ against $\log r$. When we actually try to find the fractal dimension for a set of dispersed particles, a problem occurs as to how to measure the length of the square's border. In fact, since these particles are regarded as units and the difference in the diameter of the particles is not so great, it is appropriate to define the minimum of r as a multiple of d_g. Furthermore, the increasing step size of *r* is also defined as a multiple of d_g. On the other hand, to judge whether the phase morphology has selfsimilarity, the scale function $S_M(r)$ is introduced.

$$S_M(r)=M(r)\cdot r^{-D} \tag{8}$$

As *r* increases, if $S_M(r)$ fluctuates within a small range, it means the complexity of the phase morphology does not depend on the change of *r*, or the phase morphology has selfsimilarity; then it is appropriate to study the fractal dimension.

Fractal theory by changing the coarse-graining level (called box-counting methods)

As in the previous fractal theory, we cover points distributed in space with squares whose border length is *r* and note the number of squares that contain at least one point by $N(r)$. [19,20] If $N(r)$ satisfies the relation:

$$N(r)\propto r^{-D} \tag{9}$$

When *r* changes, the distribution of points is D-dimensional, and we call D the fractal dimension. To

study the fractal behavior of the phase morphology, we cover the SEM micrograph with such squares mentioned earlier and get the corresponding $N(r)$ and r. Based on the box-counting methods, the fractal dimension can be obtained. In addition, to confirm the selfsimilarity of the phase morphology, the scale function $S_N(r)$ is defined by Formula (10).

$$S_N(r) = N(r) \cdot r^D \tag{10}$$

If $S_N(r)$ fluctuates within a small range when r changes, it means $N(r)$ is basically proportional to $r \propto^{-D}$ (the phase morphology has selfsimilarity). Thus, the fractal dimension can be obtained by plotting $\log N(r)$ against $\log r$.

EXPERIMENTAL

Materials

The basic materials used in this study were a commercial grade polyamide1010 (PA1010, 11) with a density of 1.03–1.05 g/cm^3 and a melting point of 198–210°C and a commercial grade polyethylene (PE, 5000S) with a density of 0.94–0.97 g/cm^3 and a melting point of 132–135°C. PA1010 was produced by Tianjin Zhonghe Chemical, Tianjin, China, and PE was purchased from Beijing Yanshan Petrochemical, Beijing, China.

Blends preparation

PE and PA1010 were blended in a batch internal mixer with rotor diameter of 35 mm (XXS-30 Torque rheometer produced by KeChuang Machinery, China) at 214°C. Prior to processing, all materials were dried for 8 h under vacuum at 80°C and subsequently, these predried polymers were mechanically blended in the mixer at a rotor speed of 32 rpm for 10 min. To examine the composition dependence of phase morphology of PE/PA1010 blends, various blends composition were used in this work, that is, PE/PA1010 = 10/90, 20/80, 30/70, 40/60, 50/50, 60/40, 70/30, 80/20, 90/10 wt %. After the mixing, pieces of these blends were taken out of the mixer and put into ice-water to freeze the original structure for the observation in a scanning electron microscope.

Morphological characterization

A scanning electron microscope (SEM, Philips XL30), operated at an accelerating voltage of 20 KV, was used to examine the fracture surface morphology of the blends. The preblended samples were broken in liquid nitrogen and the fracture surface was covered with gold for the observation in the microscope. To make sure the original structure of blends was intact, the surface was not etched.

The morphology was quantified using a special software. On each SEM image, the contour and mass center of each domain were detected, each domain was scanned by straight lines going through the mass center from different directions and the spans from one side of a domain to the other, which is defined as the diameter d_g in this article, were noted by a computer; consequently, the average size of the domains can be calculated by averaging these d_g using eq. (11).

$$(d_g)_m = \frac{\sum_i^\infty n_i (d_g)_i}{\sum_i^\infty n_i} \tag{11}$$

where n_i is the number of sizes. To obtain more reliable data, about 500 particles were considered to calculate these structure parameters for each sample. Considering that the quality and resolution of SEM images are strongly affected by the thickness of the plated gold, the sputter time was strictly controlled to be identical for each sample.

RESULTS AND DISCUSSION

Particle size and size distribution of blends with different compositions

Variations of typical morphologies with the composition of the PE/PA1010 blends are shown in Figure 1. At a low weight fraction of the dispersed phase, the phase morphology has the appearance of the particles in matrix and further, the particle size increases with the increasing content of the dispersed phase. When the content of PE is between 50 and 60%, the particle size is relative large and these particles deform severely so that our software could not detect the contour of each particle definitely and consequently, it is hard to determine the particle size. So, we believe that the blends have a typical cocontinuous structure when the content of PE is between 50 and 60%. Although these images show a vivid morphology, it is hard to quantitatively determine the variation of phase size just based on these images; for this reason, the particle diameter was calculated in the form of $(d_g)_m$ with a self-made software to quantitatively describe the phase size.

Figure 2 shows the variation of the average diameter $(d_g)_m$. When the concentration of the dispersed phase is low, the size of dispersed particles is small. As the concentration of dispersed phase increases, the size of the dispersed particles increases. However, one may find that this increase is not large when the content of dispersed phase is lower than 30%. It should be mentioned that, even though the different blends system is discussed in our previous

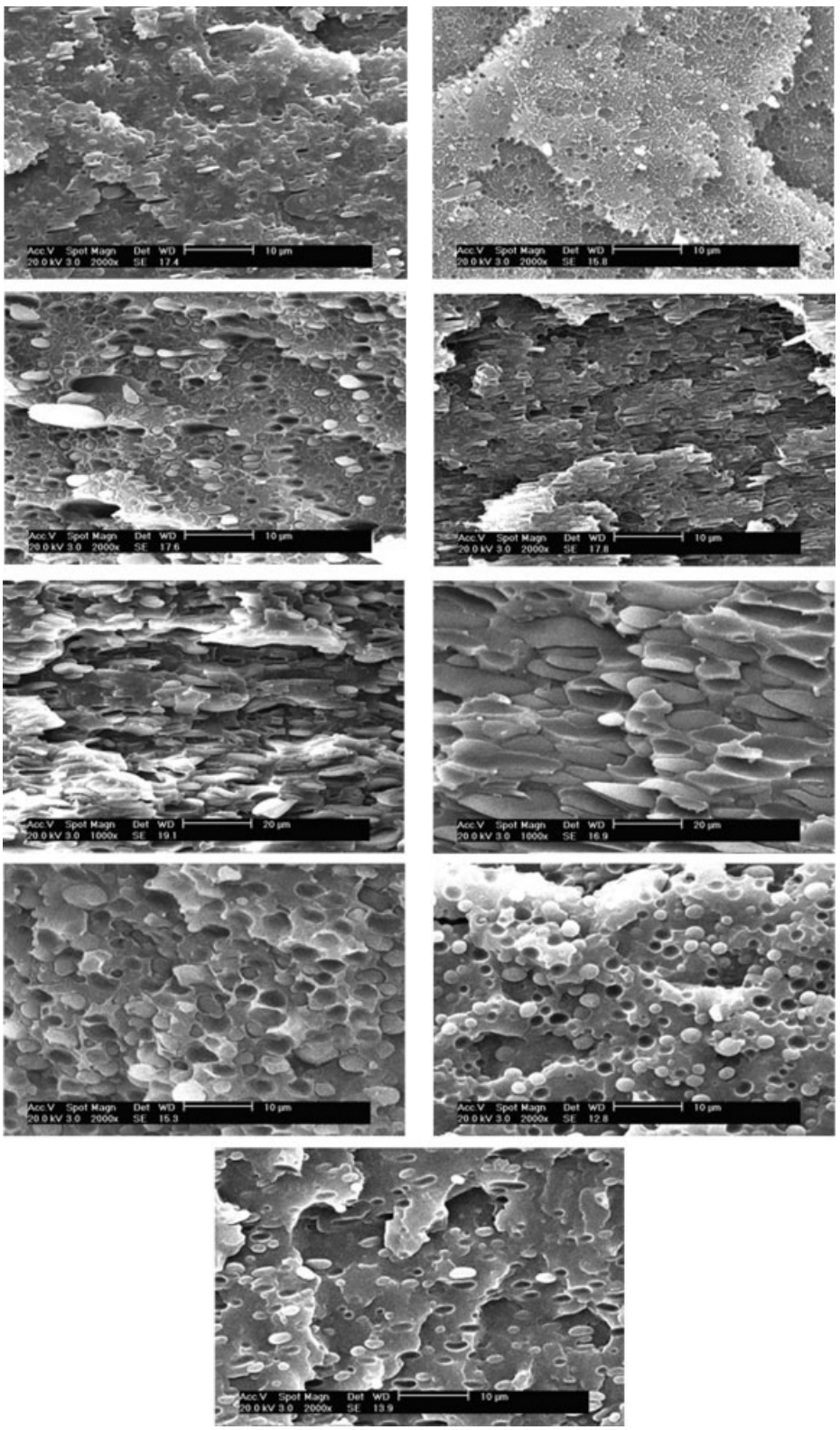

Figure 1 SEM micrographs of PE/PA1010 blends with different composition.

work, similar results were also found.[21,22] This typical result may indicate the increase in the content of dispersed phase first raised the number of domains but not their size. Only when this content is higher than 30%, the number of domains approaches to saturation and the size of these domains increases greatly. Further, we gave a quasi-quantitative model to forecast the relation between the blends composi-

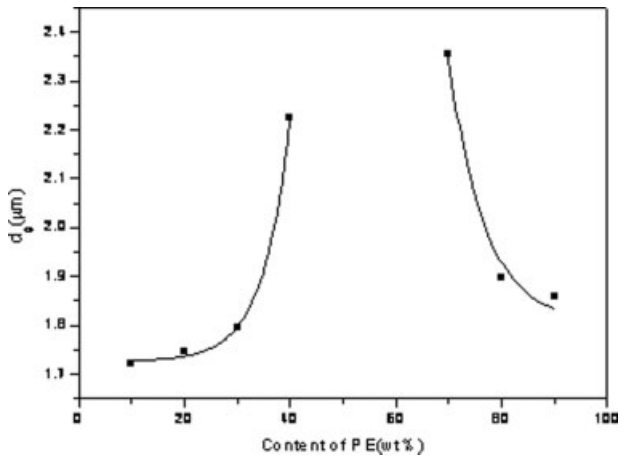

Figure 2 Variation of $(d_g)_m$ as a function of the composition of blends.

tion and corresponding morphology.[23] According to this model, when the volume fraction of the dispersed phase is small, the diameter of particles of the dispersed phase increases linearly, but when this volume fraction is relatively high, the size of particles increases more rapidly due to the coalescence effect. Despite the deficiency in this model, it shows to some extent that, when the content of dispersed phase is lower, the composition dependence of particle size is not distinct. Further, when PE is the dispersed phase, the particle size is relatively smaller than that when PA1010 is the dispersed phase, indicating that it is easier for PE to disperse in PA1010, that is, PE is prone to be the dispersed phase. For this reason, one may observe the cocontinuous region leans to the blends with high content of PA1010.

In many studies, the size distribution is discussed qualitatively.[24,25] However, it is hard to determine the distribution width of sizes quantitatively just based on the SEM micrographs. For this reason, in the theory section, the graph-estimation method is introduced to study the distribution of particle size in detail. According to this method, the distribution width of particle diameter, σ, is calculated, see Figure 3. When the content of the dispersed phase is low, the distribution width of d_g is narrow. As the content of the dispersed phase increases, due to the particle coalescence, the size of the dispersed particles and the distribution width of d_g increase. Similarly, one may observe that, when the content of the dispersed phase is less than 30%, the increase in σ is not distinct, showing that the increase in the content of the dispersed phase may not lead to a sever coalescence between particles, nor a bad deformation in particle shape. That is, the increase in the content of the dispersed phase will first lead to an increase in particle number and also, these new particles having the similar size with the original ones will dispersed into different positions in the blends rather than cluster with each other. However, when the content of the dispersed phase is more than 30%, particles begin coalescence with each other, leading to a big particle size, a severe particle deformation and a broader size distribution.

Fractal analysis of morphology of blends with different compositions

In our research team, it has been found that the spacial distribution of dispersed particles often has a significant influence on the mechanical of final blends.[26] Therefore, it is necessary to investigate the uniformity of spacial distribution of the dispersed phase. In the following part, we would like to discuss this spacial distribution by means of corresponding fractal theory which has been introduced in detailed in the theory. Based on the above-mentioned fractal theory, the scale function $S_M(r)/S_M(r)_{\max}$ and $S_N(r)/S_N(r)_{\max}$ was computed, shown in Figure 4. As r increases, both $S_M(r)/S_M(r)_{\max}$ and $S_N(r)/S_N(r)_{\max}$ fluctuate basically within a small range, which indicates the phase morphology (i.e., the spacial distribution of particles) has a selfsimilarity and consequently, the fractal dimensions, D_M and D_N, could be easily obtained to discuss the phase morphology especially the composition dependence of spacial distribution.

In Figure 5, the relation between log$M(r)$ and log$r$ mentioned in the fractal measure relations and the relation between log$N(r)$ and log$r$ mentioned in the box-counting methods were shown. As can be seen, each group of data can be approximated by a straight line. Simulating a straight line using every group of experimental data, we get the variation of the fractal dimension D as a function of the composi-

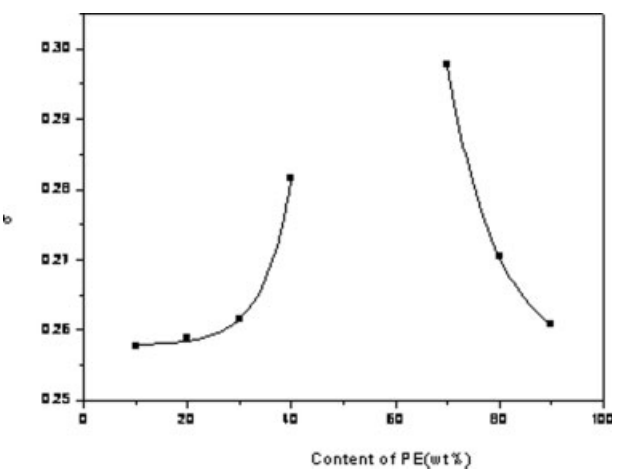

Figure 3 Variation of σ as a function of the composition of blends.

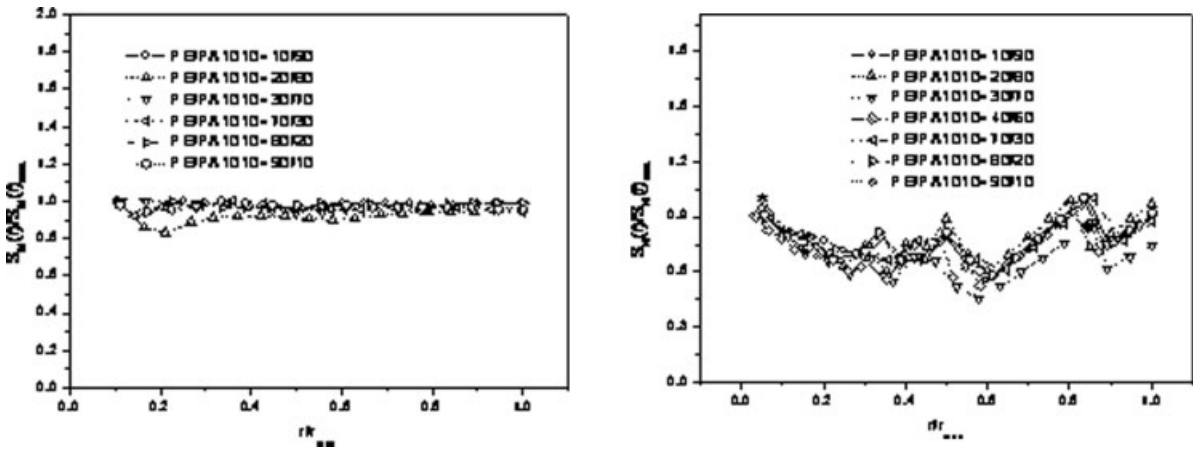

Figure 4 Scale function $S_M(r)/S_M(r)_{max}$ and $S_N(r)/S_N(r)_{max}$ with different compositions.

tion of blends, as shown in Figure 6. When the content of dispersed phase is small, the fractal dimension increases rapidly with the content. This result indicates that the particle number within in a certain area increases greatly when the content of the dispersed phase increases. Although more new particles appear in the system, it can be supposed that these new particles will rapidly disperse to different regions in the blends and further the spacial distribution of particles would be more uniform. Unfortunately, when the content of the dispersed phase is higher than 30%, the particles size is relatively large and particle number is excessive. The extra shear force of the rotor will speedup the collision and coalescence of particles, leading to a relatively nonuniform spacial distribution and a smaller fractal dimension.

From above, the fractal dimension is an effective parameter to describe the uniformity of the phase morphology and the variation of fractal dimension is related to the particle size and their distribution: when the content of the dispersed phase is lower, the particle size is smaller and there is enough space to accommodate more new particles; therefore, the increase in the content of the dispersed phase will lead to a more uniform size distribution and spacial distribution of particles. However, when the content of the dispersed phase increases, the particle size increases and inevitable coalescence will result in a nonuniform spacial distribution of particles, i.e., a smaller fraction.

Further, in the theory section, one may find that although D_M and D_N were calculated based on different methods, they have a similar physical significance. In fact, D_M and D_N should be the same. Unfortunately, we could not obtain the same value in this work. This is partially because of the inevitable calculation error. Actually, there are several parameter to characterize the spacial distribution of particles, some of these parameters have the similar meanings and are related to D_M and D_N. We would like to give a consecutive study in our other paper.

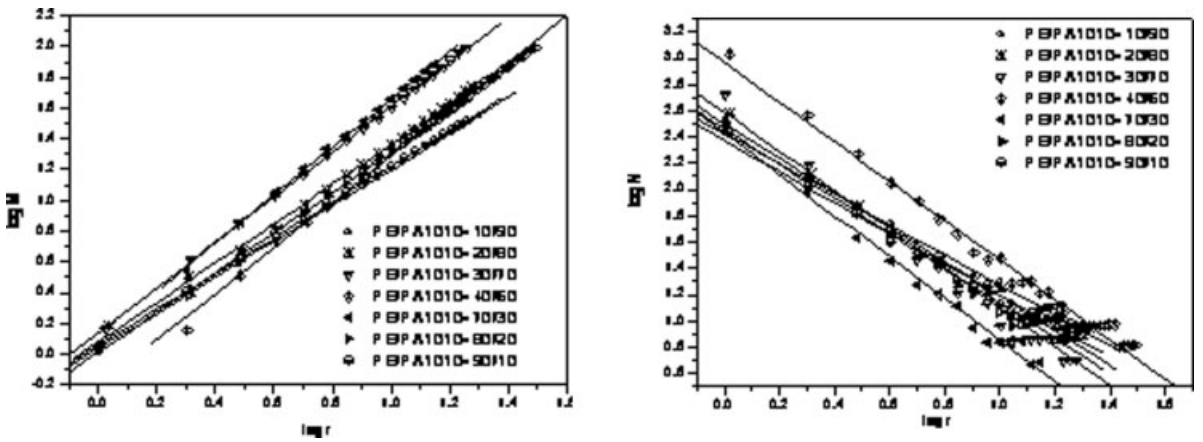

Figure 5 Relation between log$M(r)$ and log$r$, log$N(r)$ and log$r$.

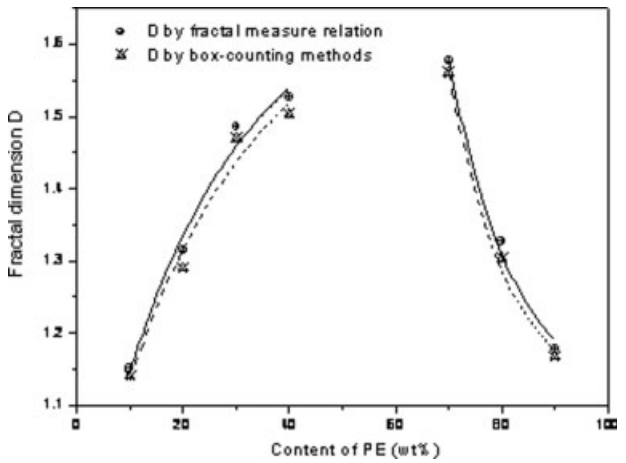

Figure 6 Variation of the fractal dimension as a function of composition of blends.

CONCLUSIONS

Composition effect on phase morphology in PE/PA blends was investigated. The results indicate that the average diameter d_g increases as the increasing content of the dispersed phase. When the proportions between the two phases are equivalent, the blends have a cocontinuous structure. Study regarding the size distribution show that, when the content of the dispersed phase is low, the distribution width of d_g is narrow. As the content of the dispersed phase increase, due to the particle coalescence, the size of the dispersed particles and the distribution width of d_g increase. The spacial distribution of dispersed particles is also studied and the results show that when the content of dispersed phase is small, the fractal dimension increases rapidly with the content and the spacial distribution is uniform. However, when the content of the dispersed phase is higher than 30%, the particles size is spacial distribution is nonuniform.

Further, the variation of all these structure parameters shows that the increase in the content of the dispersed phase will first lead to an increase in particle number and also, these new particles having the similar size with the original ones will be dispersed into different positions in the blends rather than cluster between each other. However, when the content of the dispersed phase is larger than 30%, particles begin coalescence with each other, leading to a big particle size, a severe particle deformation and a broader size distribution.

References

1. Adhikari, R.; Godehardt, R.; Lebek, W.; Michler, G. H. J Appl Polym Sci 2007, 103, 1887.
2. Lach, R.; Weidisch, R.; Knoll, K. J Polym Sci Part B: Polym Phys 2005, 43, 429.
3. Menon, A. R. R.; Sonia, T. A.; Sudha, J. D. J Appl Polym Sci 2006, 102, 5123.
4. Doshev, P.; Lohse, G.; Henning, S.; Krumova, M.; Heuvelsland, A.; Michler, G.; Radusch, H. J. J Appl Polym Sci 2006, 101, 2825.
5. Slouf, M.; Radonjic, G.; Hlavata, D.; Sikora, A. J Appl Polym Sci 2006, 101, 236.
6. Tol, R. T.; Groenincks, G.; Vinckier, I.; Moldenaers, P.; Mewis, J. Polymer 2004, 45, 2587.
7. Sailer, C.; Handge, U. A. Macromolecules 2007, 40, 2019.
8. Li, Y. Y.; Chen, Z. Q.; Huang, Y.; Sheng, J. J Appl Polym Sci 2007, 104, 666.
9. Ma, G. Q.; Zhao, Y. H.; Yan, L. T. J Appl Polym Sci 2006, 100, 4900.
10. Yang, Y. P.; Xiao, Z. G.; Jiang, X.; Sheng, J. J Macromol Sci Phys 2006, 45, 1083.
11. Chen, Y.; Sheng, J.; Shen, N. X.; Jia, H. T. Acta Polym Sin 2004, 282.
12. Plivelic, T. S.; Cassu, S. N.; Goncalves, M. D.; Torriani, I. L. Macromolecules 2007, 40, 253.
13. Jiang, C.; Filippi, S.; Magagnini, P. Polymer 2003, 44, 2411.
14. Yeh, J. T.; Chao, C. C.; Chen, C. H. J Appl Polym Sci 2000, 76, 1997.
15. Hallden, A.; Deriss, M. J.; Wessle, B. Polymer 2001, 42, 8743.
16. Poisson, C.; Hervais, V.; Lacrampe, M. F.; Krawczak, P. J Appl Polym Sci 2006, 101, 118.
17. Pan, L. H.; Chiba, T.; Inoue, T. Polymer 2001, 42, 8825.
18. Fang, K. T.; Xu, J. L. Statistics Distribution; China Science Press: Beijing, 1987; p 136.
19. Mandelbrot, B. B. Fractal Geometry of Nature; Freeman: New York, 1983; p 26.
20. Takayasu, H. Fractals in the Physical Sciences; Manchester University Press: Manchester, 1990; p 11.
21. Li, Y. Y.; Han, Y. P.; Sheng, J. J Macromol Sci Phys 2004, 43, 1175.
22. Li, Y. Y.; Guo, C.; Zhao, Y. H.; Chen, Z. Q.; Sheng, J. J Macromol Sci Phys 2007, 46, 487.
23. Zou, J. L.; Shen, N. X.; Sheng, J. Acta Polym Sin 2002, 1, 53.
24. Chen, Y.; Chen, Y.; Chen, W.; Yang, D. Eur Polym Mater 2007, 43, 2999.
25. Smit, I.; Radonjic, G.; Hlavata, D. Eur Polym Mater 2004, 40, 1433.
26. Li, Y. Y.; Han, Y. P.; Sheng, J. Chin J Polym Sci 2006, 24, 125.